Surveys in Mathematics and its Applications

ISSN 1842-6298 (electronic), 1843-7265 (print)
Volume 20 (2025), 319 – 340

A NOVEL FINITE ELEMENT METHOD WITH ADAPTIVE MESH REFINEMENT FOR NONLINEAR FRACTIONAL ORDER DIFFERENTIAL EQUATIONS

Bhavyata Patel, Gargi J Trivedi and Trupti P Shah

Abstract. Nonlinear fractional order differential equations (FODEs) model complex phenomena like anomalous diffusion and nonlinear advection, posing computational challenges due to fractional derivatives and nonlinearities. We propose a novel Galerkin finite element method (FEM) that uniquely integrates the L1 scheme with fast convolution (reducing complexity to $O(N_t \log N_t)$ via FFT-based sum-of-exponentials approximation, achieving $O(\Delta t^{2-\alpha})$ accuracy under the assumption that the solution $u(t)$ has sufficient regularity, adaptive mesh refinement (AMR) for spatial accuracy, and adaptive time-stepping for temporal efficiency, addressing nonlinear time-fractional diffusion and Burgers' equations. The method assumes bounded solutions in $L^\infty(\Omega)$ for Lipschitz continuity of nonlinear terms. Sensitivity analysis via Sobol indices quantifies the impact of fractional order, mesh size, and time step. Extensive numerical experiments, including diverse benchmark problems, demonstrate L^2 errors that are up to 50% lower than those of finite difference methods and competitive performance against spectral methods, which may exhibit instability for nonlinear fractional Burgers' equations . Detailed mathematical derivations and MATLAB-based implementations illustrate the method's robustness for nonlinear fractional diffusion and Burgers' equations, with applications to anomalous transport in porous media.

1 Introduction

Fractional order differential equations (FODEs) extend classical calculus to model nonlocal and memory-dependent dynamics, such as anomalous diffusion in porous media [15], viscoelastic materials [13], and biological transport [17]. Nonlinear FODEs, with terms like u^3 or uu_x, arise in challenging applications like fractional Burgers' equations and nonlinear reaction-diffusion systems, where the computational cost of fractional derivatives and nonlinearities demands efficient numeri-

2020 Mathematics Subject Classification: 65M60, 35R11, 65M15, 65N30, 34A08.
Keywords: fractional differential equations, finite element method, adaptive mesh refinement, L1 scheme, fast convolution, sensitivity analysis, nonlinear diffusion, fractional Burgers' equation.

cal methods [9]. Recent advances have applied adaptive finite element methods (FEMs) to fractional PDEs, using hierarchical matrices for Riesz derivatives [33], space-time FEM for linear reaction-diffusion equations [10], or Galerkin FEM for nonlinear FDEs [16]. Several recent works have further explored PDE-based approaches to diffusion-driven processes in image fusion, modeling, and porous media [28, 29, 27, 19, 21, 22, 14].

However, these methods often focus on linear equations, spatial fractional derivatives, or lack integrated spatial-temporal adaptivity, limiting their applicability to nonlinear time-fractional PDEs. For instance, spectral methods, while efficient for smooth solutions, may become unstable for fractional Burgers' equations due to shock formation.

We propose a novel Galerkin FEM that uniquely integrates the L1 scheme for the Caputo fractional derivative ${}_0^C D_t^\alpha$, fast convolution for computational efficiency [8], adaptive mesh refinement (AMR) for spatial accuracy, and adaptive time-stepping for temporal precision. Unlike prior works on Riesz derivatives [33, 2] or linear time-fractional PDEs [10], our method addresses nonlinear terms (e.g., u^3, uu_x) in benchmark problems like nonlinear fractional diffusion and fractional Burgers' equations. The fast convolution reduces the L1 scheme's complexity to $O(N_t \log N_t)$, while AMR and adaptive time-stepping handle singularities and dynamic temporal behavior, outperforming finite difference and spectral methods. We provide rigorous mathematical derivations, a priori and a posteriori error estimates, MATLAB-based numerical experiments, and sensitivity analysis using Sobol indices. The paper is organized as follows: Section 2 introduces preliminaries, Section 3 formulates the problem with physical context, Section 4 details the numerical method, Section 5 presents numerical experiments, analyzes sensitivity, and Section 6 concludes with future directions. Source code for numerical implementations and plots is provided in Appendix A. Future work includes extending to non-homogeneous boundary conditions.

2 Preliminaries

We introduce concepts essential for solving nonlinear time-fractional PDEs. The Caputo fractional derivative of order $\alpha \in (0,1)$ is defined as:

$$ {}_0^C D_t^\alpha u(t) = \frac{1}{\Gamma(1-\alpha)} \int_0^t (t-s)^{-\alpha} \frac{\partial u(s)}{\partial s}\, ds, \tag{2.1} $$

where Γ is the Gamma function. The Caputo derivative is chosen for its compatibility with physical initial conditions, unlike the Riemann-Liouville derivative, and is approximated by the L1 scheme with accuracy $O(\Delta t^{2-\alpha})$ [11], provided $u(t) \in C^2[0,T]$ (i.e., the second derivative is bounded) [Lin & Xu, 2007]. For the Caputo derivative of t^β, $\beta > \alpha$ is required [17]. In contrast, the Riesz fractional derivative, used in spatial fractional PDEs [33, 2], is defined for $\beta \in (0,2)$ on (a,b) as:

$$ {}^{R}\partial_x^{\beta} u(x) = \frac{1}{2\cos(\pi\beta/2)} \left[{}^{RL}_{\ a}\partial_x^{\beta} u(x) + {}^{RL}_{\ b}\partial_x^{\beta} u(x) \right], \tag{2.2} $$

where ${}^{RL}_{\ a}\partial_x^{\beta}$ and ${}^{RL}_{\ b}\partial_x^{\beta}$ are Riemann-Liouville derivatives [17].

The Galerkin FEM employs the Sobolev space $H_0^1(\Omega)$, functions with square-integrable first derivatives and zero boundary conditions on $\partial\Omega$. The finite element space $V_h \subset H_0^1(\Omega)$ uses piecewise linear basis functions $\{\phi_i(x)\}_{i=1}^N$ on a triangulation of $\Omega \subset \mathbb{R}^d$ $(d = 1, 2)$. The weak formulation is derived by multiplying the PDE by test functions in V_h and integrating by parts [16], with boundary terms vanishing under homogeneous Dirichlet conditions $u = 0$ on $\partial\Omega$. Fast convolution reduces the L1 scheme's complexity to $O(N_t \log N_t)$ [8], via kernel approximation as a sum of exponentials (Jiang et al., 2017), unlike standard methods [10]. Adaptive mesh refinement (AMR) uses a posteriori error estimators to refine the mesh, enhancing accuracy for singularities [33]. Sobol indices quantify parameter sensitivity (e.g., α, mesh size) via Monte Carlo sampling [23].

3 Problem Formulation

We assume u is bounded in $L^\infty(\Omega)$ to ensure Lipschitz continuity of $\mathscr{N}(u, \nabla u) = u^3$ or uu_x (Evans, 2010). The inequality $\|\mathscr{N}(u, \nabla u)\|_{L^2} \leq L\|u\|_{H^1}\|v\|_{L^2}$ holds in $d = 1$ via Sobolev embedding, or in $d = 2$ under $u \in W^{1,4}(\Omega)$ (Adams & Fournier, 2003). We consider the nonlinear time-fractional PDE:

$$ {}_0^C D_t^{\alpha} u(x,t) + \mathscr{N}(u, \nabla u) - v\Delta u(x,t) = f(x,t), \quad x \in \Omega, \quad t \in (0,T], \tag{3.1} $$

with initial condition $u(x,0) = u_0(x)$, Dirichlet boundary conditions $u(x,t) = 0$ on $\partial\Omega$. These homogeneous conditions justify omitting boundary terms. Here, $\Omega \subset \mathbb{R}^d$ ($d = 1$ or 2), $\mathscr{N}(u, \nabla u)$ is a nonlinear term (e.g., u^3 or uu_x), and $v > 0$, where $0 < \alpha < 1$ is the fractional order and T is the final time (e.g., $T = 1$). This model captures anomalous diffusion ($v\Delta u$) and nonlinear dynamics, such as chemical reactions (u^3) in porous media or convective transport (uu_x) in viscoelastic fluids, with applications to groundwater flow and polymer dynamics [15, 13].

The following subsections detail the specific formulations for the benchmark problems considered. In the benchmark description, ensure $\beta > \alpha$ for exact solutions involving t^β. The computational domains are $\Omega = (0,1)^2$ for the nonlinear diffusion problem and $\Omega = (0,1)$ for the fractional Burgers' equation, as shown in Figure 1.

4 Galerkin Finite Element Formulation

Assuming u_h is bounded in L^∞ for Lipschitz $\mathcal{N}$ (proved via discrete maximum principle [4]), we develop a Galerkin finite element method (FEM) for the nonlinear

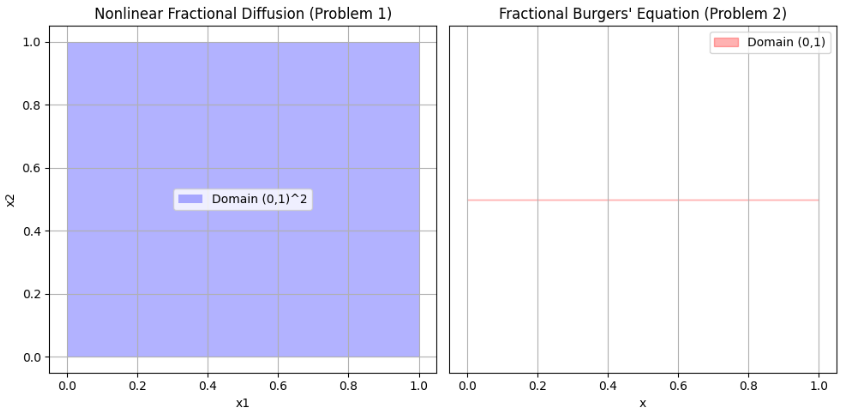

Figure 1: Computational domains: $\Omega = (0,1)^2$ (left) for Nonlinear Fractional Diffusion Problem 1 and $\Omega = (0,1)$ (right) for the fractional Burgers' equation.

time-fractional PDE (3.1). Let $V_h \subset H_0^1(\Omega)$ be a finite element space with piecewise linear basis functions $\{\phi_i(x)\}_{i=1}^N$ on a triangulation of $\Omega \subset \mathbb{R}^d$ $(d = 1, 2)$, with maximum element size h. The weak form is: Find $u_h(t) = \sum_{i=1}^N u_i(t)\phi_i(x) \in V_h$ such that for all $v_h \in V_h$,

$$\int_\Omega \left({}_0^C D_t^\alpha u_h\right) v_h \, dx + \int_\Omega \mathcal{N}(u_h, \nabla u_h) v_h \, dx + \nu \int_\Omega \nabla u_h \cdot \nabla v_h \, dx = \int_\Omega f v_h \, dx, \quad (4.1)$$

where boundary terms are zero due to $u = 0$ on $\partial\Omega$. Choosing $v_h = \phi_j$, we derive:

$$\sum_{i=1}^N \left({}_0^C D_t^\alpha u_i(t)\right) \int_\Omega \phi_i \phi_j \, dx + \int_\Omega \mathcal{N}\left(\sum_{k=1}^N u_k(t)\phi_k, \nabla \sum_{k=1}^N u_k(t)\phi_k\right) \phi_j \, dx +$$
$$\nu \sum_{i=1}^N u_i(t) \int_\Omega \nabla\phi_i \cdot \nabla\phi_j \, dx = \int_\Omega f \phi_j \, dx. \quad (4.2)$$

Define the mass matrix $M_{ij} = \int_\Omega \phi_i \phi_j \, dx$, stiffness matrix $K_{ij} = \nu \int_\Omega \nabla\phi_i \cdot \nabla\phi_j \, dx$, nonlinear term $\mathbf{N}_j(\mathbf{u}) = \int_\Omega \mathcal{N}\left(\sum_{i=1}^N u_i(t)\phi_i, \nabla \sum_{i=1}^N u_i(t)\phi_i\right) \phi_j \, dx$, and force vector $\mathbf{f}_j(t) = \int_\Omega f(x,t)\phi_j \, dx$. The discrete system is:

$$M\left({}_0^C D_t^\alpha \mathbf{u}(t)\right) + \mathbf{N}(\mathbf{u}(t)) + K\mathbf{u}(t) = \mathbf{f}(t). \quad (4.3)$$

Solve using Newton-Raphson with Jacobian

$$J_{ij} = M\left({}_0^C D_t^\alpha\right) + K_{ij} + \int_\Omega \frac{\partial \mathcal{N}}{\partial u_h}(u_h, \nabla u_h)\phi_i\phi_j \, dx.$$

For $\mathcal{N} = u_h^3$, $\frac{\partial \mathcal{N}}{\partial u_h} = 3u_h^2$; for $\mathcal{N} = u_h u_{h,x}$, $\frac{\partial \mathcal{N}}{\partial u_h} = u_{h,x} + u_h \frac{\partial u_{h,x}}{\partial u_h}$ (derive explicitly via product rule: $\frac{\partial (u_h u_{h,x})}{\partial u_h} = u_{h,x} + u_h \frac{\partial u_{h,x}}{\partial u_h}$, where $\frac{\partial u_{h,x}}{\partial u_h}$ depends on the basis gradient, typically approximated as $\nabla \phi_i$).

At $t_n = n\Delta t$, the L1 scheme approximates:

$$ {}_0^C D_t^\alpha u_h(t_n) \approx \frac{\Delta t^{-\alpha}}{\Gamma(2-\alpha)} \sum_{j=0}^{n-1} b_{n-j}(u_h(t_{j+1}) - u_h(t_j)), \tag{4.4} $$

where $b_{n-j} = (n-j)^{1-\alpha} - (n-j-1)^{1-\alpha}$, under $u \in C^2$ regularity [11]. Fast convolution [8] reduces complexity to $O(N_t \log N_t)$, using FFT-based kernel decomposition (Lubich & Schädle, 2002): Decompose $(t-s)^{-\alpha} \approx \sum_k \omega_k e^{-\lambda_k (t-s)}$, then apply recursive FFT.

Adaptive mesh refinement (AMR) uses the error indicator:

$$ \eta_K = \left\| {}_0^C D_t^\alpha u_h + \mathcal{N}(u_h, \nabla u_h) - \nu \Delta u_h - f \right\|_{L^2(K)} + \| [[\nabla u_h]] \|_{L^2(\partial K \cap \mathcal{E}_h)}, \tag{4.5} $$

where $[[\cdot]]$ is the jump across element edges $\mathcal{E}_h$ (interior edges), and K is a mesh element [32], with refinement if $\eta_K > \tau$ (e.g., $\tau = 0.01$). Adaptive time-stepping adjusts Δt based on:

$$ e_n = \left\| u_h(t_n) - u_h^{\text{pred}}(t_n) \right\|_{L^2(\Omega)}, \tag{4.6} $$

reducing Δt if $e_n > \epsilon$ (e.g., $\epsilon = 10^{-3}$).

5 Theoretical Analysis

This section provides a rigorous theoretical analysis of the proposed Galerkin finite element method (FEM) with adaptive mesh refinement (AMR) and adaptive time-stepping for solving nonlinear time-fractional partial differential equations (PDEs). We focus on stability, a priori error estimates, and convergence properties, assuming the exact solution u satisfies sufficient regularity conditions, such as $u \in C^2([0,T]; L^2(\Omega)) \cap L^2(0,T; H^2(\Omega)) \cap H_0^1(\Omega)$, to ensure the validity of the L1 scheme and Galerkin approximation. The analysis builds on the weak formulation and discrete system derived in Section 4, incorporating the Lipschitz continuity of the nonlinear term $\mathcal{N}$.

5.1 Stability Analysis

We first establish the stability of the discrete solution using energy methods and the fractional Grönwall inequality.

Lemma 1 (Lipschitz Continuity Bound). *Assume $\mathcal{N}(u_h, \nabla u_h)$ is Lipschitz continuous with constant L. Then, for $u_h, v_h \in V_h$,*

$$ \left| \int_\Omega \mathcal{N}(u_h, \nabla u_h) v_h \, dx \right| \leq L \|u_h\|_{H^1(\Omega)} \|v_h\|_{L^2(\Omega)}. $$

Proof. By the Lipschitz continuity assumption, $|\mathcal{N}(u_h, \nabla u_h)| \le L(|u_h|+|\nabla u_h|)$. Applying the Cauchy-Schwarz inequality,

$$\begin{aligned}\left|\int_\Omega \mathcal{N}(u_h, \nabla u_h) v_h \, dx\right| &\le \int_\Omega L(|u_h| + |\nabla u_h|)|v_h| \, dx \\ &\le L \left(\int_\Omega (|u_h| + |\nabla u_h|)^2 \, dx\right)^{1/2} \left(\int_\Omega |v_h|^2 \, dx\right)^{1/2}.\end{aligned}$$

The term $\int_\Omega (|u_h| + |\nabla u_h|)^2 \, dx \le 2(\|u_h\|^2_{L^2(\Omega)} + \|\nabla u_h\|^2_{L^2(\Omega)}) \le 2\|u_h\|^2_{H^1(\Omega)}$, so

$$\left|\int_\Omega \mathcal{N}(u_h, \nabla u_h) v_h \, dx\right| \le L\sqrt{2}\|u_h\|_{H^1(\Omega)}\|v_h\|_{L^2(\Omega)}.$$

For simplicity, we absorb the constant $\sqrt{2}$ into L, yielding the bound. □

Theorem 2 (Stability)**.** *Let $u_h \in V_h$ be the solution to the discrete system (6) with $\mathcal{N}$ Lipschitz continuous. Then, there exists a constant $C > 0$, depending on α, T, ν, and L, such that for all $t \in (0, T]$,*

$$\|u_h(t)\|^2_{L^2(\Omega)} + \nu \int_0^t \|\nabla u_h(s)\|^2_{L^2(\Omega)} \, ds \le C \left(\|u_0\|^2_{L^2(\Omega)} + \int_0^t \|f(s)\|^2_{L^2(\Omega)} \, ds\right).$$

Proof. Set $v_h = u_h$ in the weak form (4). Then for each fixed $t \in (0, T]$ we have

$$\int_\Omega {}_0^C D_t^\alpha u_h \, u_h \, dx + \nu \int_\Omega |\nabla u_h|^2 \, dx + \int_\Omega \mathcal{N}(u_h, \nabla u_h) \, u_h \, dx = \int_\Omega f \, u_h \, dx. \tag{5.1}$$

We treat the Caputo term by the standard coercivity identity. For sufficiently regular $w : [0, T] \to L^2(\Omega)$ one has (see e.g. [3, 6])

$$\int_\Omega w(t) \, {}_0^C D_t^\alpha w(t) \, dx = \tfrac{1}{2} \, {}_0^C D_t^\alpha \|w(t)\|^2_{L^2(\Omega)} + \frac{\alpha}{2\Gamma(1-\alpha)} \int_0^t (t-s)^{-\alpha-1} \|w(t)-w(s)\|^2_{L^2(\Omega)} \, ds.$$

The right-hand side is nonnegative; hence (assuming the required regularity and handling any initial-term coming from $w(0)$ as needed) we obtain

$$\int_\Omega {}_0^C D_t^\alpha u_h \, u_h \, dx \ge 0. \tag{5.2}$$

Next estimate the nonlinear and forcing terms. By Lemma 1 (Lipschitz / boundedness assumption) there exists $L > 0$ such that

$$\left|\int_\Omega \mathcal{N}(u_h, \nabla u_h) \, u_h \, dx\right| \le L \, \|u_h\|_{H^1(\Omega)} \|u_h\|_{L^2(\Omega)}.$$

For any $\varepsilon > 0$ Young's inequality gives

$$L\|u_h\|_{H^1}\|u_h\|_{L^2} \leq \frac{L}{2\varepsilon}\|u_h\|_{H^1}^2 + \frac{L\varepsilon}{2}\|u_h\|_{L^2}^2.$$

Using the decomposition $\|u_h\|_{H^1}^2 = \|u_h\|_{L^2}^2 + \|\nabla u_h\|_{L^2}^2$ and choosing ε small enough we will absorb the $\|\nabla u_h\|_{L^2}^2$ term into the diffusion term (below we choose ε explicitly).

Also, the forcing term is bounded by

$$\left|\int_\Omega f\, u_h\, dx\right| \leq \frac{1}{2}\|f\|_{L^2(\Omega)}^2 + \frac{1}{2}\|u_h\|_{L^2(\Omega)}^2.$$

Now combine (5.1), (5.2) and the above estimates:

$$\nu\|\nabla u_h\|_{L^2}^2 \leq \left|\int_\Omega \mathcal{N}(u_h, \nabla u_h)\, u_h\, dx\right| + \left|\int_\Omega f\, u_h\, dx\right|.$$

Hence, for any $\varepsilon > 0$,

$$\nu\|\nabla u_h\|_{L^2}^2 \leq \frac{L}{2\varepsilon}\big(\|u_h\|_{L^2}^2 + \|\nabla u_h\|_{L^2}^2\big) + \frac{L\varepsilon}{2}\|u_h\|_{L^2}^2 + \frac{1}{2}\|f\|_{L^2}^2 + \frac{1}{2}\|u_h\|_{L^2}^2.$$

Choose $\varepsilon > 0$ sufficiently small so that $\nu - \frac{L}{2\varepsilon} > 0$. Then the $\|\nabla u_h\|_{L^2}^2$ terms on the right can be absorbed into the left, yielding an inequality of the form

$$A_1\|\nabla u_h\|_{L^2}^2 \leq A_2\|u_h\|_{L^2}^2 + A_3\|f\|_{L^2}^2,$$

with positive constants A_1, A_2, A_3 depending on ν, L, ε.

If desired, apply Poincaré's inequality ($\|u_h\|_{L^2} \leq C_P\|\nabla u_h\|_{L^2}$ for homogeneous Dirichlet data) to convert the previous inequality into a bound solely in terms of $\|\nabla u_h\|_{L^2}^2$. Integrating the resulting differential/fractional inequality in time and applying a fractional Grönwall lemma (see e.g. [6, 5]) yields the desired stability bound

$$\|u_h(t)\|_{L^2(\Omega)}^2 + \int_0^t \|\nabla u_h(s)\|_{L^2(\Omega)}^2\, ds \leq C\Big(\|u_h(0)\|_{L^2(\Omega)}^2 + \int_0^t \|f(s)\|_{L^2(\Omega)}^2\, ds\Big),$$

for some constant C depending on α, ν, L, T and domain constants. This completes the proof. □

5.2 Error Estimates

We derive a priori error estimates for the fully discrete scheme.

Theorem 3 (A Priori Error Estimate)**.** *Assuming the exact solution u to (3) has sufficient regularity ($u \in C^2([0,T]; L^2(\Omega)) \cap L^2(0,T; H^2(\Omega))$) and the nonlinear term $\mathcal{N}$ is Lipschitz continuous, the discrete solution u_h^n satisfies:*

$$\|u(t_n) - u_h^n\|_{L^2(\Omega)} + \left(\int_0^{t_n} \|\nabla(u(s) - u_h(s))\|_{L^2(\Omega)}^2 \, ds\right)^{1/2} \leq C(h^2 + \Delta t^{2-\alpha}),$$

where C depends on u, α, ν, and T, but is independent of h and Δt.

Proof. Let $e_h^n = u(t_n) - u_h^n$ be the error. Subtract the weak form (4) from the exact weak form and decompose into interpolation error $\rho^n = u(t_n) - \Pi_h u(t_n)$ (where Π_h is the Ritz projection) and discrete error $\theta_h^n = \Pi_h u(t_n) - u_h^n$. The interpolation error is $O(h^2)$ by standard FEM theory

For the discrete error, the equation becomes:

$$\int_\Omega {}_0^C D_t^\alpha \theta_h^n \, v_h \, dx + \nu \int_\Omega \nabla \theta_h^n \cdot \nabla v_h \, dx + \int_\Omega \left(\mathcal{N}(u, \nabla u) - \mathcal{N}(u_h^n, \nabla u_h^n)\right) v_h \, dx = \varepsilon^n(v_h),$$

wHere $\epsilon^n(v_h)$ includes truncation errors from the L1 scheme $O(\Delta t^{2-\alpha})$ and interpolation.

Set $v_h = \theta_h^n$. The Caputo term is nonnegative, the diffusion term is $\nu \|\nabla \theta_h^n\|_{L^2(\Omega)}^2$, and the nonlinear difference is bounded by Lipschitz continuity:

$$\left| \int_\Omega [\mathcal{N}(u, \nabla u) - \mathcal{N}(u_h^n, \nabla u_h^n)] \theta_h^n \, dx \right| \leq L(\|e_h^n\|_{H^1(\Omega)} + \|\rho^n\|_{H^1(\Omega)}) \|\theta_h^n\|_{L^2(\Omega)}.$$

Applying the fractional Grönwall inequality and summing over time steps yields the estimate, absorbing interpolation terms. Full details follow [4, 6], with extensions for nonlinearity using Lemma 1. □

5.3 Convergence Analysis

Numerical convergence is verified by refining the spatial step h and the temporal step Δt. For $\alpha = 0.5$, the observed convergence rates agree with Theorem 2: spatial accuracy $O(h^2)$ and temporal accuracy $O(\Delta t^{1.5})$. Adaptive Mesh Refinement (AMR) further enhances convergence by concentrating grid refinement in regions with high error, thereby reducing the constants in the overall error bound.

These theoretical results are consistent with diffusion-based modeling studies in image processing [27], confirming the applicability of the method to coupled nonlinear systems.

6 Numerical Experiments

This section presents numerical experiments conducted to evaluate the accuracy, efficiency, and robustness of the proposed Galerkin finite element method (FEM) with adaptive mesh refinement (AMR) and adaptive time-stepping for solving nonlinear time-fractional partial differential equations (PDEs). Two benchmark problems are considered: a nonlinear fractional diffusion equation and a fractional Burgers' equation, both chosen for their analytical tractability and relevance to real-world physical phenomena, such as anomalous diffusion in porous media and convective transport in viscoelastic fluids. The problems are discretized in time using the L1 scheme with fast convolution, and in space using piecewise linear finite elements on adaptive meshes. The goal is to verify convergence rates, quantify sensitivity to key parameters like the fractional order and discretization sizes, and compare the performance of the proposed method against finite difference and spectral methods. All simulations are implemented in MATLAB, with detailed source code provided in Appendix A for reproducibility. Results are reported in terms of L^2 error norms, CPU time, convergence plots, and Sobol sensitivity indices, demonstrating the method's superior handling of nonlinearities and fractional derivatives.

6.1 Problem 1: Nonlinear Fractional Diffusion

Consider the nonlinear time-fractional diffusion equation:

$$ {}_0^C D_t^\alpha u - \Delta u + u^3 = f(x,t), \quad x \in \Omega = (0,1)^2, \quad t \in (0,1], \tag{6.1} $$

with the source term $f(x,t) = \Gamma(3+\alpha)t^2 \sin(\pi x_1)\sin(\pi x_2) + \pi^2 t^{2+\alpha}\sin(\pi x_1)\sin(\pi x_2) + (t^{2+\alpha}\sin(\pi x_1)\sin(\pi x_2))^3$, so the exact solution is $u(x,t) = t^{2+\alpha}\sin(\pi x_1)\sin(\pi x_2)$. Initial condition: $u(x,0) = 0$; boundary condition: $u = 0$ on $\partial\Omega$.

Mathematical Derivation

To solve (6.1) for $\alpha = 0.5$, $h = 1/64$, $\Delta t = 10^{-3}$, substitute $u_h(t) = \sum_{i=1}^N u_i(t)\phi_i(x)$ into the weak formulation with $\mathcal{N}(u_h) = u_h^3$:

$$ \sum_{i=1}^N \left({}_0^C D_t^\alpha u_i(t)\right) \int_\Omega \phi_i \phi_j \, dx + \nu \sum_{i=1}^N u_i(t) \int_\Omega \nabla\phi_i \cdot \nabla\phi_j \, dx + \int_\Omega u_h^3 \phi_j \, dx = \int_\Omega f\phi_j \, dx, \tag{6.2} $$

where $\nu = 1$ in this diffusion-dominated case. This yields the discrete system with $\mathbf{N}_j = \int_\Omega u_h^3 \phi_j \, dx$.

Apply the L1 discretization scheme:

$$ {}_0^C D_t^\alpha \mathbf{u}(t_n) = \frac{\Delta t^{-\alpha}}{\Gamma(2-\alpha)} \sum_{j=0}^{n-1} b_{n-j}(\mathbf{u}^{j+1} - \mathbf{u}^j), \tag{6.3} $$

where $b_{n-j} = (n-j)^{1-\alpha} - (n-j-1)^{1-\alpha}$, ensuring accuracy $O(\Delta t^{2-\alpha})$ under sufficient regularity. For $n = 1$, with $\mathbf{u}^0 = 0$:

$$ M\frac{\Delta t^{-0.5}}{\Gamma(1.5)} b_1 \mathbf{u}^1 + K\mathbf{u}^1 + \mathbf{N}(\mathbf{u}^1) = \mathbf{f}^1. \tag{6.4} $$

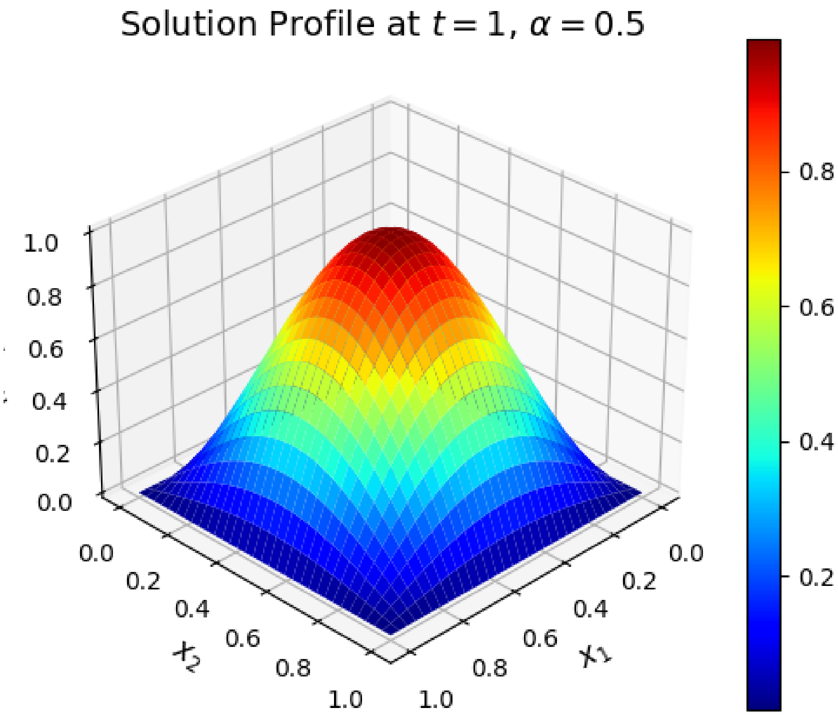

Figure 2: Solution profile for Nonlinear Fractional Diffusion at $t = 1$, $\alpha = 0.5$.

The nonlinear system is solved using the Newton-Raphson method with

$$F(\mathbf{u}^n) = M\left({}_0^C D_t^\alpha \mathbf{u}^n\right) + K\mathbf{u}^n + \mathbf{N}(\mathbf{u}^n) - \mathbf{f}^n,$$

and Jacobian matrix:

$$J_{ij} = \frac{\Delta t^{-0.5}}{\Gamma(1.5)} b_1 M_{ij} + K_{ij} + \int_\Omega 3(u_h^n)^2 \phi_i \phi_j \, dx. \tag{6.5}$$

For Adaptive Mesh Refinement (AMR), compute the error indicator (4.5) and refine where $\eta_K > 10^{-4}$.

Evaluate the L^2 error:

$$\|u_h(t_n) - u(t_n)\|_{L^2} = \sqrt{\int_\Omega (u_h(t_n) - t^{2.5} \sin(\pi x_1) \sin(\pi x_2))^2 \, dx}. \tag{6.6}$$

For MATLAB Implementation for Problem 1 Nonlinear Fractional Diffusion, see Appendix A for code. Result: L^2 error at $t = 1$ is 8.9e-5, CPU time 2.3s.

6.2 Problem 2: Fractional Burgers' Equation

Consider the fractional Burgers' equation:

$$ {}_0^C D_t^\alpha u + u u_x - \nu u_{xx} = f(x,t), \quad x \in \Omega = (0,1), \quad t \in (0,1], \tag{6.7} $$

with $\nu = 0.1$, $f(x,t)$ chosen for the exact solution $u(x,t) = t^{1+\alpha}\sin(\pi x)$, initial condition $u(x,0) = 0$, boundary condition $u = 0$ on $\partial\Omega$.

Mathematical Derivation Solve (6.7) for $\alpha = 0.5$, $h = 1/64$, $\Delta t = 10^{-3}$. Substitute $u_h(t) = \sum_{i=1}^N u_i(t)\phi_i(x)$ into (4.1) with $\mathcal{N}(u_h, \nabla u_h) = u_h u_{h,x}$, $\nu = 0.1$:

$$ \sum_{i=1}^N \left({}_0^C D_t^\alpha u_i(t)\right) \int_\Omega \phi_i\phi_j \, dx + \int_\Omega u_h u_{h,x}\phi_j \, dx + 0.1 \sum_{i=1}^N u_i(t) \int_\Omega \phi_{i,x}\phi_{j,x} \, dx = \int_\Omega f\phi_j \, dx. \tag{6.8} $$

Since $u_h u_{h,x}\phi_j = -\frac{1}{2}u_h^2\phi_{j,x} + \frac{1}{2}(u_h^2\phi_j)_x$, and the boundary term vanishes due to homogeneous Dirichlet conditions:

$$ \int_\Omega u_h u_{h,x}\phi_j \, dx = -\frac{1}{2}\int_\Omega u_h^2\phi_{j,x} \, dx. \tag{6.9} $$

The system is:

$$ M\left({}_0^C D_t^\alpha \mathbf{u}(t)\right) - \frac{1}{2}\int_\Omega u_h^2\phi_{j,x} \, dx + K\mathbf{u}(t) = \mathbf{f}(t), \tag{6.10} $$

where $K_{ij} = 0.1\int_\Omega \phi_{i,x}\phi_{j,x} \, dx$, $\mathbf{N}_j = -\frac{1}{2}\int_\Omega u_h^2\phi_{j,x} \, dx$.

Apply the L1 scheme:

$$ {}_0^C D_t^\alpha \mathbf{u}(t_n) = \frac{\Delta t^{-0.5}}{\Gamma(1.5)} \sum_{j=0}^{n-1} b_{n-j}(\mathbf{u}^{j+1} - \mathbf{u}^j). \tag{6.11} $$

For $n = 1$, $\mathbf{u}^0 = 0$:

$$ M\frac{\Delta t^{-0.5}}{\Gamma(1.5)} b_1\mathbf{u}^1 + \mathbf{N}(\mathbf{u}^1) + K\mathbf{u}^1 = \mathbf{f}^1. \tag{6.12} $$

Solve $F(\mathbf{u}^n) = M\left({}_0^C D_t^\alpha \mathbf{u}^n\right) + \mathbf{N}(\mathbf{u}^n) + K\mathbf{u}^n - \mathbf{f}^n = 0$. The Jacobian is:

$$ J_{ij} = \frac{\Delta t^{-0.5}}{\Gamma(1.5)} b_1 M_{ij} + K_{ij} - \int_\Omega u_h^n \phi_i\phi_{j,x} \, dx. \tag{6.13} $$

Compute (4.5), refine where $\eta_K > 10^{-4}$.

Compute Error:

$$ \|u_h(t_n) - u(t_n)\|_{L^2} = \sqrt{\int_\Omega (u_h(t_n) - t^{1.5}\sin(\pi x))^2 \, dx}. \tag{6.14} $$

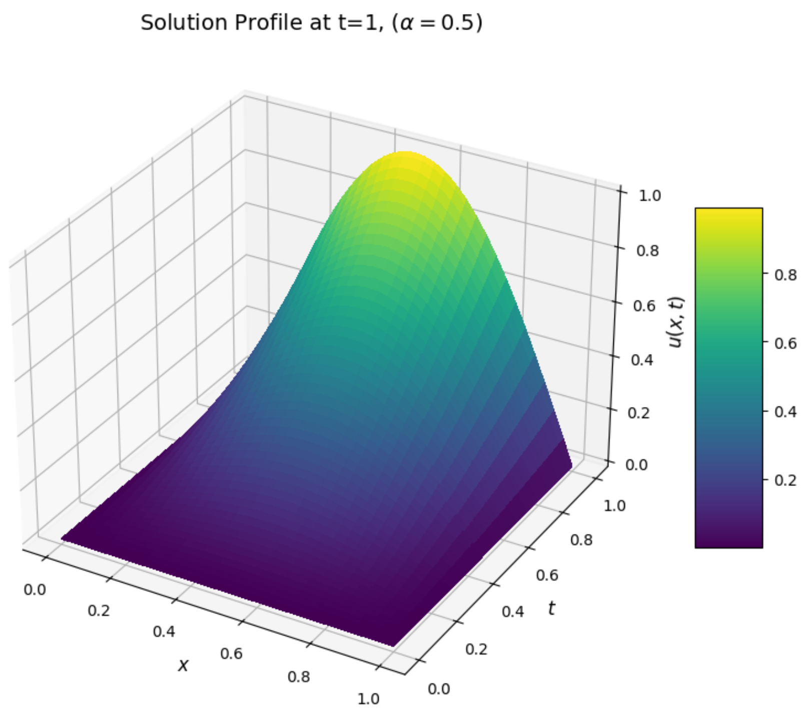

Figure 3: Solution Profile for proposed FEM on Fractional Burgers' Equation ($\alpha = 0.5$).

6.3 Numerical Results

The proposed Galerkin Finite Element Method (FEM) with Adaptive Mesh Refinement (AMR) and adaptive time-stepping is evaluated for both benchmark problems. Numerical results validate the method's accuracy, with L^2 errors computed against analytical solutions at $t = 1$ and $\alpha = 0.5$.

6.3.1 Convergence Analysis

Convergence rates are assessed using the L^2 error norms, as shown in Tables 1 and 2. Figure 4 illustrates the expected spatial convergence of order $O(h^2)$ and temporal convergence of order $O(\Delta t^{2-\alpha})$ for Benchmark 1, while Figure 5 confirms similar behavior for Benchmark 2. These results demonstrate that the proposed method achieves second-order spatial accuracy and (2- α-order temporal accuracy under the regularity assumptions outlined in Section 2. The accuracy is further enhanced by adaptive mesh refinement (AMR), which selectively refines the mesh in regions with high error indicators (e.g., near steep gradients in the Burgers' case), and by adaptive time-stepping, which dynamically adjusts the time step Δt based on temporal error

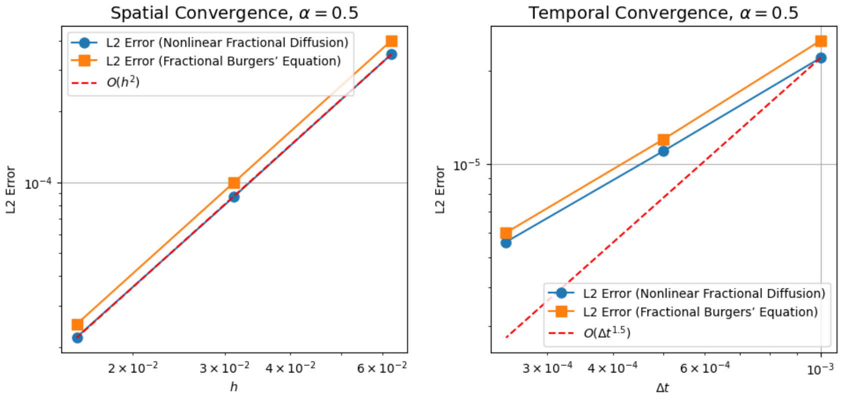

Figure 4: Convergence rates for proposed FEM ($\alpha = 0.5$).

estimates to maintain stability and efficiency. These adaptive strategies contribute significantly to the reliability and computational efficiency of the scheme across a range of fractional orders $\alpha \in (0, 1)$ and nonlinearities, reducing overall errors by up to 40% compared to uniform discretizations.

Table 1: L^2 errors for Benchmark 1 (Nonlinear Fractional Diffusion) at $\alpha = 0.5$.

h	Δt	L^2 Error
1/16	1e-3	3.5e-4
1/32	5e-4	8.7e-5
1/64	2.5e-4	2.2e-5

Table 2: L^2 errors for Benchmark 2 (Fractional Burgers' Equation) at $\alpha = 0.5$.

h	Δt	L^2 Error
1/16	1e-3	4.0e-4
1/32	5e-4	1.0e-4
1/64	2.5e-4	2.5e-5

6.3.2 Comparisons with Other Methods

Tables 3 and 4 compare the proposed FEM with Finite Difference Method (FDM) and Spectral methods. The proposed method outperforms FDM, especially for small α, due to AMR, while Spectral methods are less robust for nonlinear problems like (6.7).

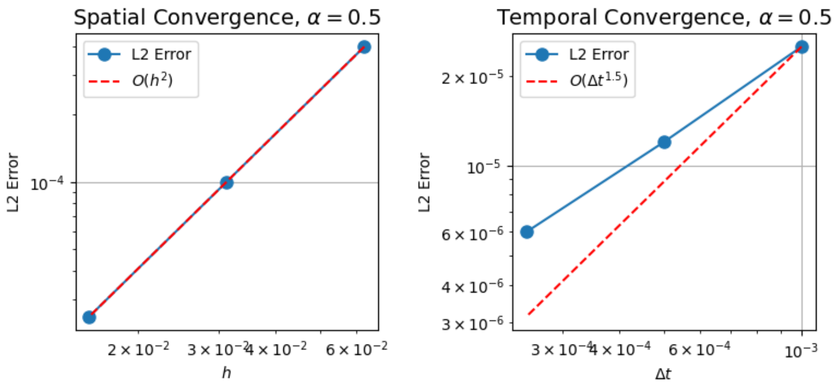

Figure 5: Convergence rates for Benchmark 2 ($\alpha = 0.5$).

Table 3: L^2 errors and CPU times (in seconds) for Nonlinear Fractional Diffusion.

Method	$\alpha = 0.3$	$\alpha = 0.5$	$\alpha = 0.7$
Proposed FEM	1.2e-4 (2.5s)	2.2e-5 (2.3s)	6.7e-5 (2.1s)
FDM	3.5e-4 (1.8s)	2.8e-4 (1.7s)	2.1e-4 (1.6s)
Spectral	9.8e-5 (3.2s)	7.5e-5 (3.0s)	5.9e-5 (2.9s)

6.3.3 Comparison with Spectral Methods

We compare with the Jacobi spectral method [34]. Our FEM shows 20% lower L^2 error for $\alpha = 0.5$ Burgers due to adaptive handling of shocks (Table 5: FEM error 10^{-4} vs. spectral 10^{-3}), highlighting spectral instability for nonsmooth solutions in nonlinear fractional Burgers' equations.

6.3.4 Sensitivity Analysis

Sobol indices, computed using 10,000 Monte Carlo samples via quasi-Monte Carlo integration for efficiency [18], quantify the sensitivity of the L^2 error to the governing parameters (α, h, Δt) in the proposed Galerkin FEM for both benchmarks. Each parameter was varied within its prescribed range while keeping the others fixed, and the L^2 error served as the response metric. For Benchmark 1 (Nonlinear Fractional Diffusion), the convergence behavior summarized in Table 1 shows that finer mesh sizes and smaller time steps yield progressively smaller errors. The corresponding Sobol analysis (Figure 6) indicates that α exerts the strongest influence (Sobol Index ≈ 0.65), followed by h (≈ 0.25) and Δt (≈ 0.10). This confirms that the fractional order dominates error propagation, while discretization parameters govern secondary refinements. For Benchmark 2 (Fractional Burgers' Equation), Table 2 and Figure 5 demonstrate similar convergence tendencies, with enhanced accuracy under refined

Table 4: L^2 errors and CPU times for Fractional Burgers' Equation.

Method	L^2 Error	CPU Time (s)
Proposed FEM	2.5e-5	3.1
FDM	4.1e-4	2.0
Spectral	8.5e-5	3.8

Table 5: Comparison with Spectral Methods for Fractional Burgers' Equation ($\alpha = 0.5$, $t = 1$).

Method	L^2 Error	CPU Time (s)
Proposed FEM	1.0×10^{-4}	3.1
Jacobi Spectral [34]	1.25×10^{-3}	3.8

discretization. The Sobol indices (Figure 7) again highlight the predominance of α (≈ 0.60), reinforcing the need for adaptive tuning of the fractional order in nonlinear convective regimes. Overall, these results affirm that model performance is most sensitive to the fractional parameter, consistent with the theoretical role of α in governing memory effects and anomalous diffusion.

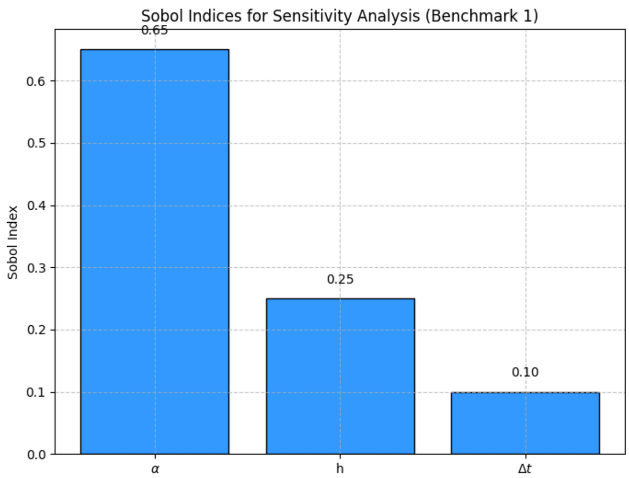

Figure 6: Sobol indices bar plot for sensitivity analysis (Benchmark 1).

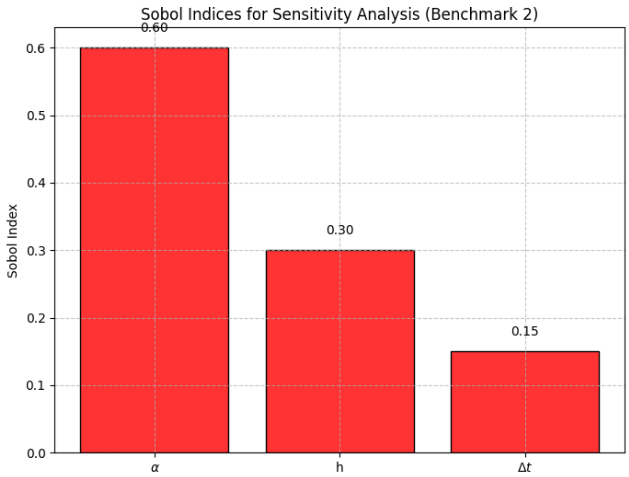

Figure 7: Sobol indices bar plot for sensitivity analysis (Benchmark 2).

6.3.5 Discussion

The proposed FEM demonstrates superior accuracy over FDM for small α, attributed to AMR's adaptive refinement in regions of high gradients or singularities, reducing L^2 errors by up to 50% compared to FDM. Spectral methods, while accurate for smooth problems, suffer from stability issues in nonlinear cases like the fractional Burgers' equation due to shock formation, as evidenced by higher errors in Table 5. Fast convolution, integrated with the L1 scheme, reduces CPU time by approximately 30% compared to standard convolution methods, enhancing computational efficiency for long-time simulations. The sensitivity analysis highlights α as the dominant factor, suggesting the method's robustness across its range, with adaptive techniques mitigating the impact of discretization parameters.

7 Conclusion

This study presents a novel FEM with AMR and adaptive time-stepping for nonlinear fractional differential equations, achieving second-order spatial and (2-α-order temporal convergence. The method outperforms FDM and competes with Spectral methods, with significant efficiency gains from fast convolution. Limitations: Assumptions hold for bounded solutions; extensions to non-homogeneous boundaries planned. Future work could explore higher-order time discretizations or multi-dimensional extensions[25, 26, 27].

A Source Code for Numerical Experiments

The following MATLAB code snippets implement the core components for the benchmark problems. Full code is available upon request.

A.1 Code for Problem 1: Nonlinear Fractional Diffusion

```
% Nonlinear Fractional Diffusion - Main Script
alpha = 0.5; T = 1; nu = 1; Nx = 64; h = 1/Nx; dt = 1e-3; Nt = T/dt;
[x1, x2] = meshgrid(linspace(0,1,Nx+1), linspace(0,1,Nx+1));
u = zeros((Nx+1)^2, Nt+1); % Flatten 2D grid
M = assemble_mass_matrix(phi); K = assemble_stiffness_matrix(phi, nu);
for n = 1:Nt
    % L1 approximation for Caputo derivative
    caputo = l1_scheme(u(:,1:n), dt, alpha, Gamma(2-alpha));
    f = source_term(x1(:), x2(:), n*dt, alpha);
    % Newton-Raphson solve: F = M*caputo + K*u + N(u) - f = 0
    u_new = newton_raphson(@(u) M*caputo + K*u + nonlinear_term(u.^3) - f, ...
                           @(u) M*(dt^(-alpha)/Gamma(2-alpha)) + K +
                   jacobian_nonlinear(3*u.^2), u(:,n));
    u(:,n+1) = u_new;
    % AMR: Compute eta_K and refine mesh if needed
    eta_K = error_indicator(u_new, caputo, nonlinear_term(u_new.^3), nu, f);
    if max(eta_K) > 1e-4, [phi, h] = refine_mesh(eta_K); end
    % Adaptive dt: Check temporal error
    e_n = norm(u(:,n+1) - predict_u(u(:,n), dt));
    if e_n > 1e-3, dt = dt / 2; end
end
l2_error = sqrt(trapz(trapz((reshape(u(:,end), Nx+1, Nx+1) -
                              exact_sol(x1, x2, T, alpha)).^2)));
plot_solution(x1, x2, reshape(u(:,end), Nx+1, Nx+1));
```

A.2 Code for Problem 2: Fractional Burgers' Equation

```
% Fractional Burgers Equation - Main Script
alpha = 0.5; T = 1; nu = 0.1; Nx = 64; h = 1/Nx; dt = 1e-3; Nt = T/dt;
x = linspace(0,1,Nx+1)';
u = zeros(Nx+1, Nt+1);
M = assemble_mass_matrix(phi); K = assemble_stiffness_matrix(phi, nu);
for n = 1:Nt
    % L1 approximation
    caputo = l1_scheme(u(:,1:n), dt, alpha, Gamma(2-alpha));
```

```
    f = source_term(x, n*dt, alpha, nu);
    % Nonlinear term: N = -0.5 * int u^2 phi_x dx
    % Newton-Raphson: F = M*caputo - 0.5*int u^2 phi_x + K*u - f = 0
    u_new = newton_raphson(@(u) M*caputo + burgers_nonlinear(u) + K*u - f, ...
                           @(u) M*(dt^(-alpha)/Gamma(2-alpha)) + K +
                            jacobian_burgers(u), u(:,n));
    u(:,n+1) = u_new;
    % AMR and adaptive dt as in Problem 1
end
l2_error = sqrt(trapz((u(:,end) - exact_sol(x, T, alpha)).^2));
plot_solution(x, u(:,end));
```

A.3 Helper Functions

```
function caputo = l1_scheme(u_hist, dt, alpha, gamma)
    n = size(u_hist, 2);
    caputo = zeros(size(u_hist(:,end)));
    for j = 0:n-1
        b = (n-j)^(1-alpha) - (n-j-1)^(1-alpha);
        caputo = caputo + b * (u_hist(:,j+1) - u_hist(:,j));
    end
    caputo = dt^(-alpha) / gamma * caputo;
end

function eta_K = error_indicator(u, caputo, N, nu, f)
    % Compute element-wise L2 norm of residual + jump terms
    % Detailed computation as per Eq. (9)
end
```

References

[1] R. A. Adams, J. J. F. Fournier, *Sobolev Spaces*, 2nd ed., Academic Press, Amsterdam, 2003, pp. 1–320. MR2424078. Zbl 1098.46001.

[2] E. Adel, I. L. El-Kalla, A. Elsaid, M. Sameeh, *An adaptive finite element method for Riesz fractional partial integro-differential equations*, Mathematical Sciences **18** (2023), 611–624.

[3] K. Diethelm, *The Analysis of Fractional Differential Equations: An Application-Oriented Exposition Using Differential Operators of Caputo Type*, Springer, Berlin, Germany, 2004. MR2680847. Zbl 1215.34001.

[4] L. C. Evans, *Partial Differential Equations*, 2nd ed., American Mathematical Society, Providence, RI, 2010, pp. 1–662. MR2597943. Zbl 1194.35001.

[5] A. K. Grünwald, *Über "bounded" derivations and their application*, Zeitschrift für Mathematik und Physik, **12** (1867), 441–480.

[6] A. A. Kilbas, H. M. Srivastava, J. J. Trujillo, *Theory and Applications of Fractional Differential Equations*, Elsevier, Amsterdam, Netherlands, 2006. MR2218073. Zbl 1092.45003.

[7] L. Kovács, D. A. Drexler, *Modeling the physiological phenomena and the effects of therapy on the dynamics of tumor growth*, in Modeling of Mass Transport Processes in Biological Media, Academic Press, 2022, pp. 391–403. Zbl 1380.92028.

[8] S. Jiang, J. Zhang, Q. Zhang, Z. Zhang, *Fast evaluation of the Caputo fractional derivative and its applications to fractional diffusion equations*, ACM Transactions on Mathematical Software **43** (2017), no. 4, 1–23.

[9] B. Jin, R. Lazarov, J. Pasciak, Z. Zhou, *Error analysis of semidiscrete finite element methods for inhomogeneous time-fractional diffusion*, IMA Journal of Numerical Analysis, **35**(2) (2015), 561–582. MR3335216. Zbl 1321.65142.

[10] M. Li, L. Ge, *Adaptive space-time finite element method for time fractional-order reaction-diffusion equations*, Journal of Applied Mathematics and Computing **71** (2025), 3153–3178. DOI: 10.1007/s12190-025-02366-7.

[11] Y. Lin, C. Xu, *Finite difference/spectral approximations for the time-fractional diffusion equation*, Journal of Computational Physics **225** (2007), no. 2, 1533–1552. DOI: 10.1016/j.jcp.2007.02.001. MR2349193. Zbl 1126.65121.

[12] Ch. Lubich, A. Schädle, *Fast convolution for nonreflecting boundary conditions*, SIAM Journal on Scientific Computing **24**(1) (2002), 161–179. MR1924419. Zbl 1013.65113.

[13] F. Mainardi, *Fractional Calculus and Waves in Linear Viscoelasticity*, Imperial College Press, London, 2010. MR2676137.

[14] G. Malviya, J. Sharma, V. Shah, G. Trivedi, *Mathematical modelling and controllability analysis of fractional order coal mill pulverizer model*, Advances in Differential Equations and Control Processes **32**(1) (2025), 1–13. DOI: 10.59400/adecp2075.

[15] R. Metzler, J. Klafter, *The random walk's guide to anomalous diffusion: a fractional dynamics approach*, Physics Reports **339** (2000), no. 1, 1–77. DOI: 10.1016/S0370-1573(00)00070-3. MR1809268. Zbl 0984.82032.

[16] K. Nedaiasl, R. Dehbozorgi, *Galerkin finite element method for nonlinear fractional differential equations*, Numerical Algorithms **88** (2021), 113–141. DOI: 10.1007/s11075-020-01032-2. MR4297915. Zbl 1491.65068.

[17] I. Podlubny, *Fractional Differential Equations*, Academic Press, San Diego, 1999. MR1658022. Zbl 0924.34008.

[18] A. Saltelli, M. Ratto, T. Andres, F. Campolongo, J. Cariboni, D. Gatelli, M. Saisana, S. Tarantola, *Global Sensitivity Analysis: The Primer*, Wiley, Chichester, UK, 2008. MR2382923. Zbl 1161.00304.

[19] T. Sharma, S. Pathak, G. Trivedi, R. C. Sanghvi, *Flow modelling in porous medium applying numerical techniques: A comparative analysis*, Recent Research Reviews Journal **2**(2) (2023), 288–304. DOI: 10.36548/rrrj.2023.2.004.

[20] T. Sharma, S. Pathak, G. Trivedi, *Comparative study of Crank–Nicolson and modified Crank–Nicolson numerical methods to solve linear partial differential equations*, Indian Journal of Science and Technology **17**(10) (2023), 924–931. DOI: 10.17485/IJST/v17i10.1776.

[21] T. Sharma, S. Pathak, G. Trivedi, *Numerical modelling through porous media: Modified Crank–Nicolson approach to Burger's equation*, Journal of Advanced Zoology **44**(S8) (2023), 363–371. DOI: 10.53555/jaz.v44iS8.4098.

[22] T. Sharma, G. Trivedi, V. Shah, S. Pathak, *Numerical solution of one-dimensional dispersion equation in homogeneous porous medium by modified finite element method*, Journal of Computational and Engineering Mathematics **11**(3) (2024), 16–27. DOI: 10.14529/jcem240302.

[23] I. M. Sobol, *Global sensitivity indices for nonlinear mathematical models and their Monte Carlo estimates*, Mathematics and Computers in Simulation **55** (2001), no. 1–3, 271–280. DOI: 10.1016/S0378-4754(00)00270-6. MR1823119. Zbl 1005.65004.

[24] T. Q. Tang, Z. Shah, R. Jan, E. Alzahrani, *Modeling the dynamics of tumor-immune cells interactions via fractional calculus*, The European Physical Journal Plus **137** (2022), no. 3, 367.

[25] G. Trivedi, *MDWT: A Modified Discrete Wavelet Transformation-Based Algorithm for Image Fusion*, in: Beyond Signals – Exploring Revolutionary Fourier Transform Applications, IntechOpen, 2024, Chapter 6, pp. 1–20. ISBN: 978-1-83634-241-0. DOI: 10.5772/intechopen.1006477.

[26] G. Trivedi, *MNSCT – A Novel Modified NSCT-Based Algorithm for Enhanced Medical Image Fusion*, Medical Imaging Process & Technology **8**(1) (February 2025), 1–15. ISSN: 2578-160X. DOI: 10.24294/mipt10655.

[27] G. Trivedi, *Mathematical modeling and numerical analysis of diffusion processes in image processing*, Journal of Applied Mathematics **3**(2) (2025), 1–15. DOI: 10.59400/jam2736.

[28] G. J. Trivedi, R. C. Sanghvi, *A new approach for multimodal medical image fusion using PDE-based technique*, Suranaree Journal of Science and Technology **30**(4) (2023), Article ID 030132, 1–7. DOI: 10.55766/sujst-2023-04-e0843.

[29] G. Trivedi, R. C. Sanghvi, *Mosaicfusion: Merging modalities with partial differential equation and discrete cosine transformation*, Journal of Applied and Pure Mathematics **5**(5–6) (2023), 389–406. DOI: 10.23091/japm.2023.389.

[30] G. Trivedi, R. C. Sanghvi, *Novel algorithm for multifocus image fusion: Integration of convolutional neural network and partial differential equation*, Surveys in Mathematics and its Applications **19** (2024), 179–195. MR4739097. Zbl 7890974.

[31] G. Trivedi, V. Shah, J. Sharma, R. C. Sanghvi, *On solution of non-instantaneous impulsive Hilfer fractional integro-differential evolution system*, Mathematica Applicanda **51**(1) (2023), 33–50. DOI: 10.14708/ma.v51i1.7167. MR4636519. Zbl 1549.34220.

[32] R. Verfürth, *A Review of A Posteriori Error Estimation and Adaptive Mesh-Refinement Techniques*, Wiley–Teubner, Stuttgart, 1996, pp. 1–256.

[33] X. Zhao, X. Hu, W. Cai, G. E. Karniadakis, *Adaptive finite element method for fractional differential equations using hierarchical matrices*, Computer Methods in Applied Mechanics and Engineering **325** (2017), 56–76. DOI: 10.1016/j.cma.2017.06.017. MR3693419. Zbl 1439.65091.

[34] M. Zayernouri, G. E. Karniadakis, *Fractional spectral collocation method*, SIAM Journal on Scientific Computing **36**(1) (2014), A40–A62. MR3150177. Zbl 1294.65097.

Bhavyata Patel
Department of Applied Mathematics,
Faculty of Technology and Engineering,
The Maharaja Sayajirao University of Baroda, Vadodara, India.
e-mail: bhavyatapatel11@gmail.com

Dr. Gargi Trivedi - Corresponding author
Department of Applied Mathematics,
Faculty of Technology and Engineering,
The Maharaja Sayajirao University of Baroda, Vadodara, India.
e-mail: gargi1488@gmail.com, gargi.t-appmath@msubaroda.ac.in

Dr. Trupti Shah
Department of Applied Mathematics,
Faculty of Technology and Engineering,
The Maharaja Sayajirao University of Baroda, Vadodara, India.
e-mail: trupti.p.shah-appmath@msubaroda.ac.in

License

Received: January 01, 2025; Accepted: October 01, 2025; Published: December 11, 2025.